BIOMOLECULES & THERAPEUTICS

Original Article
Biomol Ther 32(1), 84-93 (2024)

Rosmarinic Acid Inhibits Ultraviolet B-Mediated Oxidative Damage via the AKT/ERK-NRF2-GSH Pathway *In Vitro* and *In Vivo*

Mei Jing Piao[1,†], Pattage Madushan Dilhara Jayatissa Fernando[1,†], Kyoung Ah Kang[1], Pincha Devage Sameera Madushan Fernando[1], Herath Mudiyanselage Udari Lakmini Herath[1], Young Ree Kim[2,*] and Jin Won Hyun[1,*]

[1]*Department of Biochemistry, College of Medicine, and Jeju Research Center for Natural Medicine, Jeju National University, Jeju 63243,*
[2]*Department of Laboratory Medicine, Jeju National University Hospital, and College of Medicine, Jeju National University, Jeju 63241, Republic of Korea*

Abstract

Rosmarinic acid (RA) is a phenolic ester that protects human keratinocytes against oxidative damage induced by ultraviolet B (UVB) exposure, however, the mechanisms underlying its effects remain unclear. This study aimed to elucidate the cell signaling mechanisms that regulate the antioxidant activity of RA and confirm its cyto-protective role. To explore the signaling mechanisms, we used the human keratinocyte cell line HaCaT and SKH1 hairless mouse skin. RA enhanced glutamate-cysteine ligase catalytic subunit (GCLC) and glutathione synthetase (GSS) expression in HaCaT cells in a dose- and time-dependent manner. Moreover, RA induced nuclear factor erythroid-2-related factor 2 (NRF2) nuclear translocation and activated the signaling kinases protein kinase B (AKT) and extracellular signal-regulated kinase (ERK). Treatment with the phosphatidylinositol 3-kinase (PI3K) inhibitor LY294002, the ERK inhibitor U0126, and small interfering RNA (siRNA) gene silencing suppressed RA-enhanced GCLC, GSS, and NRF2 expression, respectively. Cell viability tests showed that RA significantly prevented UVB-induced cell viability decrease, whereas the glutathione (GSH) inhibitors buthionine sulfoximine, LY294002, and U0126 significantly reduced this effect. Moreover, RA protected against DNA damage and protein carbonylation, lipid peroxidation, and apoptosis caused by UVB-induced oxidative stress in a concentration-dependent manner in SKH1 hairless mouse skin tissues. These results suggest that RA protects against UVB-induced oxidative damage by activating AKT and ERK signaling to regulate NRF2 signaling and enhance GSH biosynthesis. Thus, RA treatment may be a promising approach to protect the skin from UVB-induced oxidative damage.

Key Words: Glutathione, NRF2, Oxidative damage, Rosmarinic acid (RA)

INTRODUCTION

The skin provides the first physical barrier against the external environment and is frequently exposed to various challenges that induce oxidative stress, including toxic chemicals, mechanical injuries, and environmental stress factors such as ultraviolet (UV) radiation. Collectively, these stressors trigger irreversible biomolecular damage to the skin, thereby inducing carcinogenesis and cell senescence (Papaccio *et al*., 2022). Solar UV radiation, the most frequently found carcinogen in the environment, causes premature aging and induces the formation of reactive oxygen species (ROS) (McDaniel *et al*., 2018), oxidative damage to cellular macromolecules, immunosuppression, and inflammation (Liu *et al*., 2022b). Upon exposure to sunlight, endogenous chromophores present in the skin initiate the conversion of sunlight photons to ROS. Although ROS have important physiological functions in cell signaling, enzymatic reactions, and resistance against microbes, their excessive levels can be toxic unless they are removed in a timely manner (Wang *et al*., 2023). As keratinocytes form

Open Access **https://doi.org/10.4062/biomolther.2023.179**

Received Oct 13, 2023 **Revised** Nov 15, 2023 **Accepted** Nov 16, 2023
Published Online Jan 1, 2024

***Corresponding Authors**
E-mail: namu8790@jejunu.ac.kr (Kim YR), jinwonh@jejunu.ac.kr (Hyun JW)
Tel: +82-64-717-1456 (Kim YR), +82-64-754-3838 (Hyun JW)
Fax: +82-64-717-1456 (Kim YR), +82-64-702-2687 (Hyun JW)
[†]The first two authors contributed equally to this work.

the outermost layer of the skin and are frequently exposed to stressful stimuli, sophisticated cyto-protective functions likely play an important role in maintaining their proper functions in this tissue. In this context, cells depend on dynamic detoxification mechanisms, which can be achieved by distinct detoxification enzymes as well as ROS quenchers with low molecular weights, such as carotenoids, polyphenols, and vitamins C and E.

Reduced form of glutathione (GSH), a highly abundant tripeptide formed by glutamate, cysteine, and glycine in all cell types, has attracted considerable interest in cancer prevention and chemo-resistance. GSH acts as a redox buffer and alleviates the toxicity of endogenous and exogenous electrophilic agents. It also plays a crucial role in apoptosis and its levels are associated with caspase activity (Liu *et al*., 2022a). GSH is thought to function in the transcriptional activity of many genes, including those involved in ceramide production, Bcl-2 protein expression, and thiol redox signaling (He *et al*., 2020; Wang *et al*., 2020; Gonchar *et al*., 2021; Nie *et al*., 2023). Additionally, reduced GSH levels facilitate oxidative stress and cancer progression (Azmanova and Pitto-Barry, 2022). γ-Glutamyl cysteine ligase, the rate-limiting enzyme that enhances cysteine uptake in GSH biosynthesis, is regulated by nuclear factor erythroid-2-related factor 2 (NRF2), a redox-sensitive transcription factor (Kumar *et al*., 2022). Activation of the NRF2 pathway upregulates phase II enzyme genes in response to oxidative stress, thereby protecting against oxidative stress (G Bardallo *et al*., 2022). Therefore, compounds that can stimulate the NRF2-antioxidant response element pathway as GSH-boosting agents have gained increasing attention in treating various diseases governed by oxidative stress.

Plant-derived phytochemicals, such as sulforaphane, resveratrol, and curcumin, stimulate cell stress-induced maintenance and enhance repair mechanisms via the induction of NRF2 in the skin (Ashrafizadeh *et al*., 2020; Farkhondeh *et al*., 2020; Wei *et al*., 2021). Rosmarinic acid (RA) is a phenolic ester and a promising natural compound in a variety of medicinal plant species, including rosemary (*Rosmarinus officinalis L.*), lemon balm (*Melissa officinalis L.*), spearmint (*Mentha spp.*), and several Chinese herbal plants (Amoah *et al*., 2016). It exhibits several pharmacological and biological activities, including antioxidant, anti-inflammatory, anti-apoptotic, anti-fibrotic, and anti-bacterial effects (Li *et al*., 2010; Rocha *et al*., 2015; Noor *et al*., 2022; Ijaz *et al*., 2023). Furthermore, our previous study reported the cyto-protective efficacy of RA in response to ultraviolet B (UVB) radiation-induced cellular oxidative damage by enhancing its antioxidant properties (Fernando *et al*., 2016). Thus, RA appears to offer cellular protection to the skin, however, the underlying mechanisms and fundamental cell signaling pathways have not yet been elucidated. In this study, we explored the cell signaling mechanisms that regulate the antioxidant activity of RA and confirmed its cyto-protective role, *in vivo*, against UVB-induced oxidative damage in SKH1 hairless mouse skin.

MATERIALS AND METHODS

Reagents

RA was purchased from Santa Cruz Biotechnology (Dallas, TX, USA). 3-(4,5-Dimethylthiazol-2-yl)-2,5-diphenyltetrazolium bromide (MTT), buthionine sulfoximine (BSO), padimate O, and actin antibody were purchased from Sigma-Aldrich (St. Louis, MO, USA). Glutamate-cysteine ligase catalytic subunit (GCLC), glutathione synthetase (GSS), phospho-NRF2, and TATA-binding protein (TBP) antibodies were purchased from Abcam (Cambridge, MA, USA). Phospho-histone H2A.X, phospho-protein kinase B (AKT), AKT, caspase-3, and poly ADP-ribose polymerase (PARP) antibodies were purchased from Cell Signaling Technology (Danvers, MA, USA). The superoxide dismutase (SOD) 1 antibody was purchased from Enzo Life Sciences (Farmingdale, NY, USA). Antibodies against NRF2, catalase (CAT), Bax, Bcl-2, caspase-9, extracellular signal-regulated kinase (ERK) 2, and phospho-ERK were purchased from Santa Cruz Biotechnology. LY294002 and U0126 were purchased from Calbiochem (San Diego, CA, USA). Cell Tracker™ Blue CMAC dye was obtained from Molecular Probes (Eugene, OR, USA). All the other chemicals and reagents were of analytical grade.

Cell culture and UVB exposure

The human keratinocyte cell line (HaCaT), which was provided by Cell Lines Service GmbH (Eppelheim, Germany), was maintained at 37°C in an incubator with a humidified atmosphere of 5% CO_2 and 95% air. Cells were cultured in Dulbecco's modified Eagle's medium containing 10% fetal calf serum, streptomycin (100 μg/mL), and penicillin (100 units/mL). The cells were irradiated with UVB light at 30 mJ/cm^2. The UVB light source and irradiation method have been previously reported (Piao *et al*., 2015).

Skin tissue preparation

The *in vivo* experiments were conducted using hairless mice (SKH1 hairless mice, 7 weeks old) obtained from Orient Bio Inc. (Seongnam, Korea). Mice were maintained in cages, which were installed in a temperature-controlled room with 12 h light/12 h dark cycles, and were provided with *ad libitum* access to water and standard food. Experimental procedures involving animals and their handling were performed in accordance with the guidelines established for the care and use of laboratory animals at Jeju National University (Jeju, Korea). Male mice, each weighing 20-30 g, were randomly divided into 5 groups with 5 mice each: non-irradiated control, UVB-irradiated control, RA (0.01 mg/mL and 0.1 mg/mL, respectively)-treated irradiated group, and padimate O (5 mM)-treated irradiated group. Padimate O is a US Food and Drug Administration-approved sunscreen agent that can be used in all types of cosmetics (Pantelic *et al*., 2023). Thus, we used padimate O as a positive control reagent. Before UVB irradiation, a sterile cotton swab containing RA or padimate O was evenly applied to the back of the mouse 3 times a week for 15 weeks. Mice were irradiated with a UVP UV lamp (UVP. LLC. Upland, CA, USA) for 4 min and 35 sec to reach 100 mJ/cm^2. The UVB dose was quantified using an HD2102.2 instrument (Delta Ohm Srl, Caselle di Selvazzano, Italy). Dorsal skin samples with full skin thickness were rapidly collected from the middle back area of the skin and frozen at −80°C until further processing for gene expression and enzyme activity measurements.

Reverse transcription-PCR (RT-PCR)

Easy-BLUE™ total RNA extraction kit (iNtRON Biotechnology Inc., Seongnam, Korea) was used to isolate the total RNA

out of the human keratinocytes. Reverse transcription of total RNA to cDNA was achieved by using 1 μL of reverse transcription reaction buffer, primers, dNTPs, and 0.5 U of Taq DNA polymerase in a final volume of 20 μL. PCR was performed under the following conditions: 94°C for 5 min; 26 cycles of 94°C for 30 sec; 63°C for 45 sec; 72°C for 1 min; 72°C for 7 min. The used primer pairs were as follows (forward and reverse, respectively): GCLC, 5′-AACCAAGCGCCATGCCGACC-3′ and 5′-CCTCC TTCCGGCGTTTTCGC-3′; GSS, 5′-GCCCCATTCACGCTCTTCCCC-3′ and 5′-ATGCCCGGCCTGCTTAGCTC-3′; GAPDH, 5′-TCAAGTGGGGCGATGCTGGC-3′, and 5′-TGCCAGCCCCAGCGTCAAAG-3′. The blue/orange 6 × loading dye was diluted with the resulting PCR products to track DNA migration. The final mixture was resolved by electrophoresis on a 1% agarose gel, stained with ethidium bromide, and photographed under ultraviolet light using ImageQuant TL analysis software (Amersham Biosciences, Uppsala, Sweden).

Western blotting analysis

The cells were harvested and washed twice with ice-cold PBS. The resulting cell pellets were lysed with 120 μL of protein lysis buffer (PRO-PREP protein extraction solution (iNtRON Biotechnology Inc.) in ice for 30 min and centrifuged at 13,000×g for 5 min to collect the supernatants. For mouse tissues, even-sized skin samples were first washed with PBS and then lysed in PRO-PREP protein extraction solution (iNtRON Biotechnology Inc.) for 30 min with frequent homogenization. The tissue lysates were centrifuged at 13,000×g for 5 min. Supernatants were collected and protein concentrations were quantified. Aliquots of around 30 μg of protein were boiled for 5 min and resolved in 10% SDS-polyacrylamide gels. Proteins were transferred to a nitrocellulose membrane, blocked with 3% bovine serum albumin solution at 20°C for 1 h, and subjected to incubation with appropriate primary antibodies overnight at 4°C. The membranes were then incubated with horseradish peroxidase-conjugated anti-immunoglobulin G (Pierce, Rockford, IL, USA). The protein bands were detected using an enhanced chemi-luminescence western blot detection kit (Amersham Biosciences, Little Chalfont, Buckinghamshire, UK).

Immunocytochemistry

Cells were plated at 1.0×10^5 cells/well in a four-well chamber slide. Sixteen hours after seeding, the cells were treated with RA (2.5 μM) and incubated for 12 h. Cells were fixed with 100% ethanol for 10 min, permeabilized with 0.1% Triton X-100 in PBS for 30 min, and washed with PBS three times. Subsequently, cells were treated with a blocking medium containing 5% BSA in PBS for 1 h at 37°C and then exposed to an anti-NRF2 antibody diluted in blocking medium (1:125 dilution) overnight. A FITC-conjugated secondary antibody (diluted 1:500) was added and incubated for 1 h to detect the immune-oreactive primary NRF2 antibody. Excess antibodies were washed away with PBS, and the stained cells were mounted onto microscope slides in a mounting medium containing DAPI for nuclear counterstaining. Images were captured using a FluoView FV1200 laser-scanning confocal microscope (Olympus Life Sciences, Tokyo, Japan).

Transient transfection of small interfering RNA (siRNA)

Cells were seeded at 1.0×10^5 cells/mL in 24 well plates and allowed to grow to approximately 50% confluence. The siRNA construct was a mismatched siRNA control (siControl; Santa Cruz Biotechnology). siRNAs against AKT (siAKT; Bioneer, Seoul, Korea), and ERK1 (siERK1; Santa Cruz Biotechnology) were used. Following the manufacturer's instructions, Lipofectamine™ 2000 (Invitrogen, Carlsbad, CA, USA) was employed to transfect cells along with 10-50 nM siRNA. Subsequently, cells were treated with 2.5 μM RA and incubated for 24 h for western blot analysis.

Detection of GSH levels

Cell cultures (1.0×10^5 cells/mL) were treated with 2.5 μM RA and exposed to UVB 1 h later. Following 24 h of incubation, cells were treated with 10 μM of CMAC dye, and samples were incubated for a further 30 min at 37°C. Additional dye was washed off with PBS, and the stained cells were mounted onto a chamber slide in a mounting medium. The slides were observed under a confocal microscope using the LSM 5 PASCAL software (Carl Zeiss, Jena, Germany). GSH levels were determined by spectrophotometry in either cells or mouse tissues using a BIOXYTECH GSH-400 assay kit (Oxis International Inc., Foster City, CA, USA) following the manufacturer's protocol.

Cell viability

Cells were seeded in 24 well plates at a density of 1×10^5 cells/mL for 16 h, pretreated with 10 μM BSO (an inhibitor of GSH), 5 μM LY294002 (an inhibitor of phosphatidylinositol 3-kinase (PI3K)/AKT), or 10 nM U0126 (an inhibitor of ERK kinase) and incubated for 1 h before treatment with RA at 2.5 μM. Cells were subsequently exposed to UVB and incubated for 24 h at 37°C, and MTT solution was added (125 μM per well). Following a 4 h incubation period, the supernatants were aspirated and 350 μL of dimethyl sulfoxide was added to dissolve the formazan crystals in the wells. Finally, the absorbance was measured at 540 nm using a VersaMax ELISA Microplate Reader (Molecular Devices, Sunnyvale, CA, USA).

Detection of 8-hydroxy-2′-deoxyguanosine (8-OHdG)

DNA was isolated from mouse skin using a Wizard genomic DNA purification kit (Promega, Madison, WI, USA) and quantified using a spectrophotometer. The levels of 8-OHdG present in DNA isolated from mouse skin tissues were assayed using a Bioxytech 8-OHdG-ELISA kit (OXIS Health Products, Portland, OR, USA), according to the manufacturer's instructions.

Protein carbonylation

Protein carbonylation was measured using an Oxiselect™ protein carbonyl ELISA kit (Cell Biolabs, San Diego, CA, USA), following the manufacturer's instructions.

Lipid peroxidation

The levels of isoprostane were measured using an OxiSelect™ 8-iso-prostaglandin F2α ELISA kit (Cell Biolabs), according to the manufacturer's protocol.

Statistical analysis

All measurements were performed in triplicate, and data are presented as the mean ± the standard error (SE). Data were statistically analyzed using one-way analysis of variance, followed by Tukey's test to analyze the difference. Statistical significance was set at $p<0.05$.

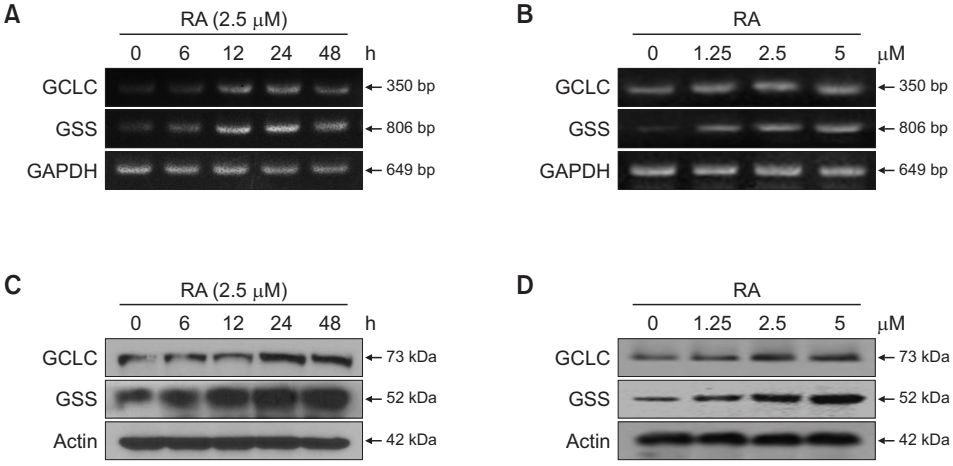

Fig. 1. Rosmarinic acid (RA) increases the mRNA and protein expression of glutamate-cysteine ligase catalytic subunit (GCLC) and glutathione synthetase (GSS) in human HaCaT keratinocytes. Cells were treated with RA for 0, 6, 12, 24, and 48 h at 2.5 μM or 1.25, 2.5, and 5 μM for 24 h respectively. (A, B) mRNA expression of GCLC and GSS was analyzed by reverse transcription-PCR (RT-PCR). (C, D) Protein expression levels of GCLC and GSS were assessed by western blot.

RESULTS

RA upregulates the mRNA and protein expression levels of GCLC and GSS

Cells were treated with 2.5 μM RA for 0, 6, 12, 24, and 48 h or RA at different concentrations (1.25, 2.5, and 5 μM) for 24 h. The relative mRNA expression of GCLC and GSS increased in a time- and dose-dependent manner (Fig. 1A, 1B). The peak mRNA expression level was reached at 24 h (Fig. 1A), with 2.5 and 5 μM of RA inducing the highest mRNA levels (Fig. 1B). Similarly, the ability of RA to induce GCLC and GSS protein expression was assessed using western blotting. As shown in Fig. 1C and 1D, GCLC and GSS protein levels in the cells were increased by RA treatment in a time- and concentration-dependent manner. Therefore, treatment with 2.5 μM RA for 24 h was considered the optimal treatment for subsequent experiments.

RA increases the levels of NRF2 transcription factor and induces the AKT and ERK pathways

To determine whether RA activated NRF2, the nuclear fraction of NRF2 was measured at the indicated time points. Western blotting showed that RA remarkably increased phospho-NRF2 and NRF2 levels in the nuclear fraction after 6 and 12 h of incubation (Fig. 2A). Furthermore, RA facilitated the translocation of NRF2 from the cytosol to the nucleus (Fig. 2B). Various kinases, such as PI3K, ERK, JNK, and p38, mediate the phosphorylation of NRF2 (Liu *et al*., 2021). To investigate the upstream signaling pathways that dominate RA-induced NRF2 activation, we analyzed the involvement of AKT and ERK, which are both well-known signaling enzymes that protect cells against oxidative stress. Therefore, the phosphorylation of AKT and ERK upon incubation with RA was analyzed via western blotting using specific antibodies. As shown in Fig. 2C and 2D, treatment with RA activated AKT and ERK signaling in a time-dependent manner.

AKT and ERK pathways are involved in RA-induced NRF2 expression and cytoprotection against UVB radiation

To confirm the involvement of AKT and ERK in the activation of NRF2, we treated cells with LY294002 (a PI3K/AKT inhibitor) and U0126 (an ERK kinase inhibitor) for 1 h, followed by the addition of RA and incubation for 12 h (optimal time for NRF2 activation) or 24 h (optimal time for GSS and GCLC activation) to investigate protein expression levels. The levels of phosphorylated AKT and ERK in the RA + inhibitor group were significantly lower than those in the RA-treated group (Fig. 3A). Moreover, GCLC and GSS protein expression levels were elevated following RA treatment, whereas they were notably decreased after treatment with LY294002 and U126 (Fig. 3B). To further investigate the contribution of AKT and ERK signaling, AKT and ERK gene expression was disrupted using small interfering RNA (siRNA). The results were consistent with the use of the inhibitors (Fig. 3C). In addition, the RA-induced increase in phospho-NRF2 and NRF2 levels were significantly diminished in the presence of LY294002 and U0126 (Fig. 3D). Therefore, this experimental evidence is consistent with the involvement of the PI3K/AKT and ERK pathways in the activation of NRF2 to induce GSH expression. To determine whether the cyto-protective effects of RA were dependent on the activation of the AKT and ERK signaling pathways, cell viability was examined by the MTT assay. The results showed that RA, LY294002, and U0126 were not cytotoxic, whereas UVB radiation caused an extreme decrease in cell viability. However, RA was able to protect cells against the cytotoxicity caused by UVB. Notably, LY294002 and U0126 reversed this effect (Fig. 3E).

GSH participates in the protective effect of RA on UVB-induced cell damage

GSH plays a vital role in the maintenance of cellular antioxidant systems, as well as in a range of metabolic processes via the regulation of intracellular redox balance (Jena *et al*., 2023). Therefore, the protein expression of GSS and GCLC was measured using western blotting. RA markedly prevented the UVB-induced downregulation of GCLC and GSS protein

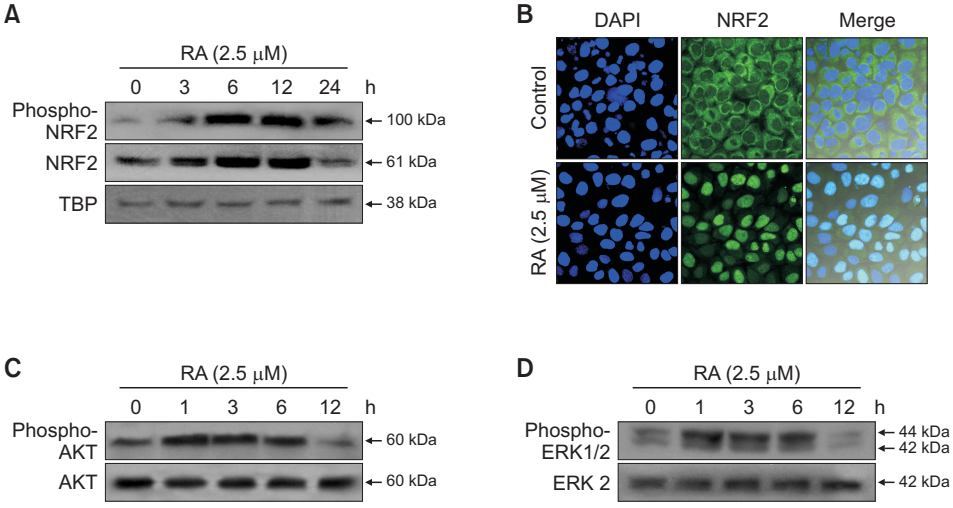

Fig. 2. Rosmarinic acid (RA) induces the nuclear accumulation of nuclear factor erythroid-2-related factor 2 (NRF2), protein kinase B (AKT), and phosphorylation of extracellular signal-regulated kinase (ERK) in human HaCaT keratinocytes. Cells were pretreated with 2.5 μM of RA for 0 to 24 h (3, 6, 12, and 24 h), and the nuclear extract was prepared following the harvest at certain time points. (A) NRF2 activation at different time passages was assessed using western blot analysis using NRF2 and phospho-NRF2 antibodies. TATA-binding protein (TBP) was used as a loading control protein. (B) Intracellular NRF2 localization in cultured cells was assessed via immunocytochemistry using an anti-NRF2 antibody and a FITC-conjugated secondary antibody. Nuclei stained with DAPI appear blue, and NRF2 localization appears green. (C, D) Cells were incubated with 2.5 μM of RA for 0 to 12 h (1, 3, 6, 12 h) intervals, proteins were extracted for western blot, and (C) phospho-AKT, AKT, (D) phospho-ERK, ERK2, were detected using specific antibodies.

expression levels (Fig. 4A). Next, we tested whether RA up-regulated cellular GSH levels upon UVB irradiation. Cellular GSH levels were assessed using confocal microscopy and staining with a specific dye, CMAC, which indicates the presence of GSH. Fluorescence intensity was higher in RA-treated cells, whereas GSH expression was not detected in the UVB-treated group. Notably, pretreatment with RA inhibited the UVB-induced reduction in GSH levels (Fig. 4B). In addition, the cellular GSH levels were measured using a commercially available GSH detection kit. As shown in Fig. 4C, while RA increased GSH levels, the increase was not significant; however, it significantly suppressed the reduction in GSH levels caused by exposure to UVB. The association between GSH and RA-induced cyto-protection was assayed in the presence of the specific GSH inhibitor BSO. Cell viability was significantly reduced in the UVB-treated group and RA pretreatment greatly increased cell viability. However, BSO significantly attenuated the RA-enhanced cell viability (Fig. 4D). Therefore, RA-induced cyto-protection against UVB irradiation is achieved via modulation of cellular GSH levels.

RA attenuates UVB-induced macromolecular damage in mouse skin tissue

We have previously demonstrated that RA protects human HaCaT keratinocytes against UVB-induced macromolecular damage (Fernando *et al*., 2016). Therefore, we examined whether this effect occurred *in vivo*. Phosphorylation of H2A.X is a sensitive marker for evaluating DNA damage because phosphorylation of H2A.X at Ser 139 is a rapid and abundant phenomenon related to double-strand breakages (Li *et al*., 2021). As shown in Fig. 5A, treatment with RA (0.01 or 0.1 mg/mL) or treatment with the positive control padimate O significantly reduced UVB-induced H2A.X phosphorylation. In addition, UVB radiation significantly induced the production of 8-OHdG, which is the most stable and abundant product of oxidative DNA damage. However, RA treatment attenuated this increase (Fig. 5B). Additionally, the formation of carbonyl groups is a marker of protein oxidation and is enhanced by ROS. There was a significant increase in protein carbonyl formation in UVB-irradiated mice skin, which was inhibited by RA at 0.01 and 0.1 mg/mL concentrations, or padimate O (Fig. 5C). The levels of 8-isoprostane, a reliable candidate for photo-oxidative damage, were evaluated (Vetrani *et al*., 2022). Consistent with our previous results, 8-isoprostane formation was observed in the UVB-irradiated control group, whereas treatment with RA or padimate O decreased the 8-isoprostane levels (Fig. 5D). Most importantly, in each case, the reduction in oxidative damage was higher in the high-dose RA (0.1 mg/mL) treatment group than in the low-dose RA (0.01 mg/mL) treatment group, thus implying that RA prevents cellular macromolecular damage and safeguards the skin from UVB irradiation-induced damage in a dose-dependent manner.

RA protects against UVB radiation-induced antioxidant enzyme imbalance and apoptosis in mouse skin tissue

We examined the effect of RA on intracellular antioxidant enzyme activity after UVB irradiation *in vitro* (Fernando *et al*., 2016). To confirm this hypothesis, we investigated the effect *in vivo*. We measured the protein levels of CAT and SOD1. As shown in Fig. 6A, RA treatment significantly increased CAT and SOD1 protein levels in the skin tissues of mice exposed to UVB radiation, and this effect was more prominent at high RA concentrations. UVB radiation causes severe damage to the skin; in response, cells continue their repair mechanisms or undergo apoptosis to tolerate the damage. The protein levels of Bax, cleaved caspase-9 and caspase-3, and cleaved PARP, which is an indicator of mitochondria-mediated apoptosis, were significantly higher in UVB-treated mouse skin tis-

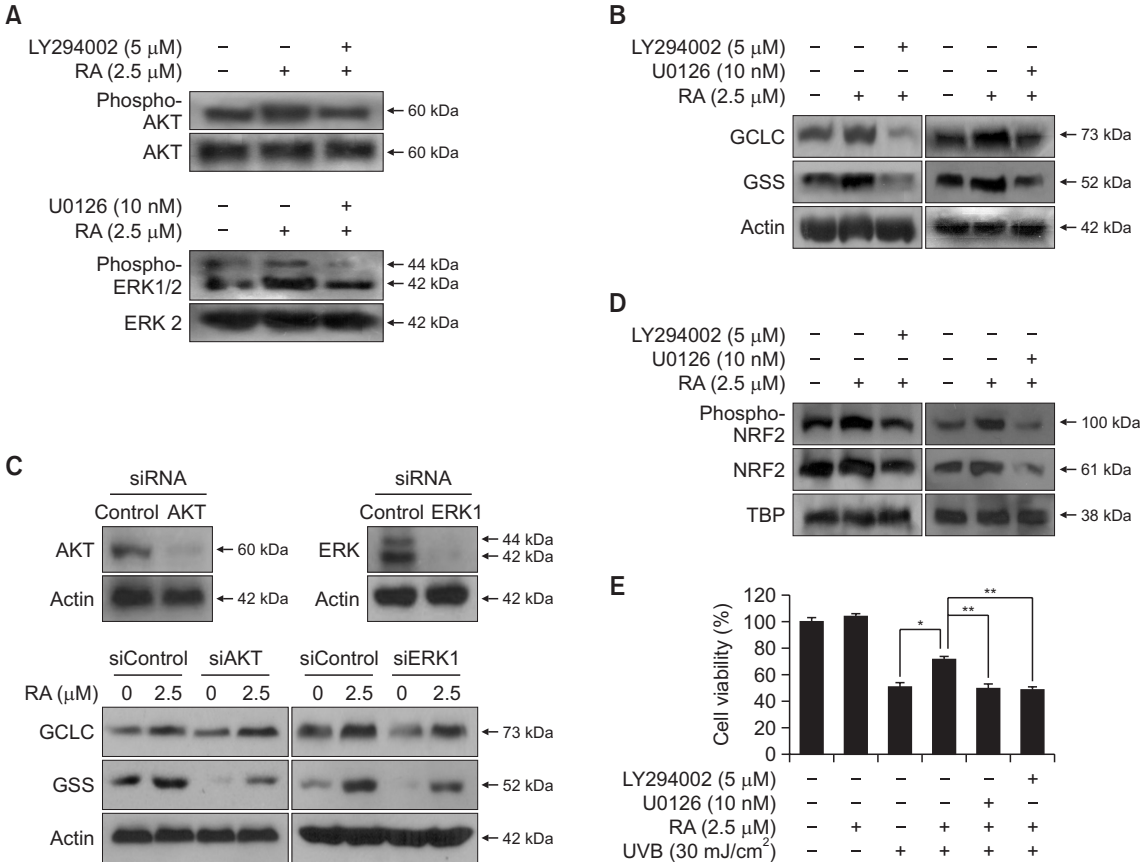

Fig. 3. Phosphorylation of protein kinase B (AKT) and extracellular signal-regulated kinase (ERK) is involved in the induction of glutamate-cysteine ligase catalytic subunit (GCLC) and glutathione synthetase (GSS) and activation of nuclear factor erythroid-2-related factor 2 (NRF2) in human HaCaT keratinocytes. (A, B) Cells were treated with LY294002 (PI3K/AKT inhibitor) or U0126 (ERK inhibitor), and following 1 h, RA was added. And (A) phospho-AKT, AKT or phospho-ERK, ERK2, and (B) GCLC, GSS protein expressions were determined by western blot analysis. Cells were transfected with 20 nM siControl and siAKT or siERK1. After 16 h of incubation, cells were treated with RA (2.5 μM) for 24 h. (C) Effect of siAKT or siERK1 on the expression of GCLC and GSS was observed via western blot using specific antibodies. (D) Cells were incubated with LY294002 or U0126, treated with RA (2.5 μM). Phospho-NRF2 and NRF2 protein expressions were detected by their specific antibodies. The TBP antibody was used as a loading control for nuclear proteins. (E) Cells were incubated with LY294002 or U0126, treated with RA (2.5 μM), and exposed to UVB for the detection of cell viability using the MTT assay. *Significantly different from UVB-treated cells (p<0.05), and **significantly different from RA plus UVB-treated cells (p<0.05).

sue, and anti-apoptotic Bcl-2 protein expression was reduced. However, RA significantly reduced the protein expression of each apoptosis marker, which was consistent with our previous *in vitro* observations (Fig. 6B).

RA protection against UVB radiation is achieved by regulating NRF2-GSH signaling *in vivo*

To improve the accuracy of the *in vitro* results, GCLC, GSS, and GSH synthesis indicators and protein expression were evaluated in mouse dorsal skin tissue to verify the involvement of GSH in the subsequent NRF2 activation. Compared with the UVB-irradiated group where the expression of the GCLC and GSS proteins was remarkably reduced, the RA-treated groups (0.01 or 0.1 mg/mL) exhibited increased GCLC and GSS expression levels, which is consistent with the effect of the positive control padimate O (Fig. 7A). The dose of UVB irradiation used in this experiment drastically reduced the GSH levels in the skin tissue, whereas treatment with 0.01 or 0.1 mg/mL RA and the positive control padimate O restored this UVB-induced GSH depletion in a significant manner (Fig. 7B). Furthermore, RA upregulated the expression and translocation of NRF2 into the nucleus in a dose-dependent manner (Fig. 7C).

DISCUSSION

The epidermis, the outermost layer of the skin, is surrounded by keratinocytes, which are frequently exposed to a range of harmful external stimuli, such as UV radiation (Mohamed and Hargest, 2022). The oxidative stress caused by these environmental factors has numerous deleterious effects on the skin. To counterbalance these detrimental effects, mammalian cells have oxidative stress-tolerant pathways, particularly the NRF2 transcription factor, which is activated by oxidative and electrophilic stress. NRF2 regulates the expression of a wide array of genes encoding phase II antioxidant enzymes, such as SOD, CAT, and NAD(P)H quinone oxidoreductase (Galicia-Moreno *et al*., 2020).

RA is a naturally occurring herbal extract that enhances cel-

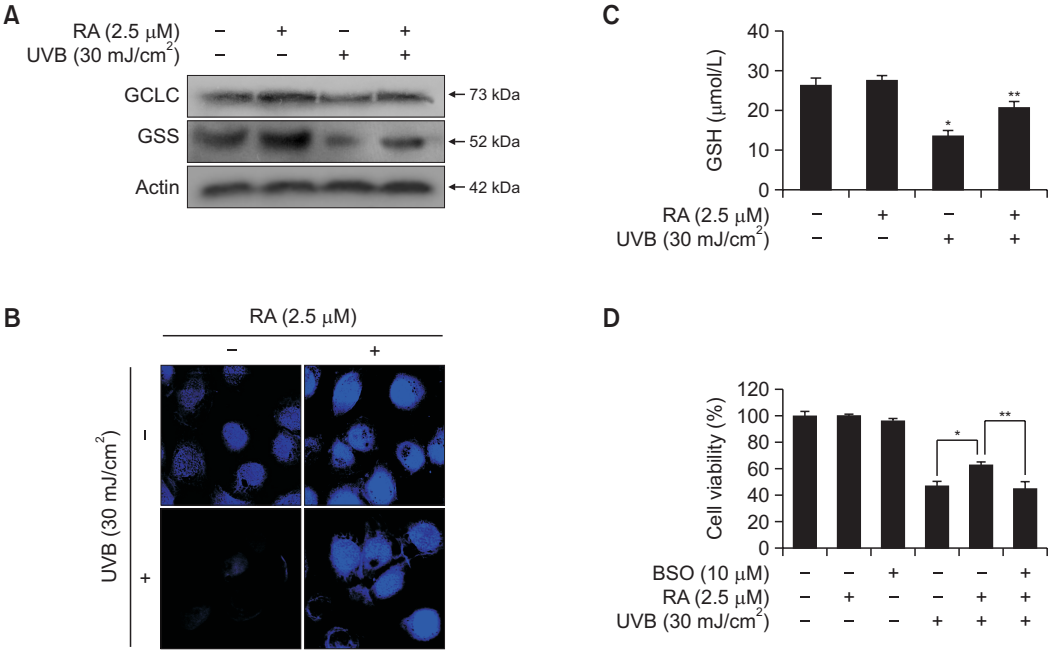

Fig. 4. Rosmarinic acid (RA) alleviates the reduction in glutathione (GSH) levels induced by UVB radiation in human HaCaT keratinocytes. Cells were pretreated with RA (2.5 μM) and then exposed to UVB and incubated for 24 h. (A) The protein expressions of GCLC and GSS were detected by western blot analysis. Actin was used as a loading control. (B) After cells were stained with CMAC, a specific dye for GSH detection, GSH levels were detected using confocal microscopy. (C) GSH levels were measured using a commercial GSH detection kit. *Significantly different from control (p<0.05), **significantly different from UVB-irradiated cells (p<0.05). (D) Cells were incubated with GSH inhibitor buthionine sulfoximine (BSO), treated with RA (2.5 μM), and exposed to UVB for analysis of cell viability using the MTT assay. *Significantly different from UVB-treated cells (p<0.05), and **significantly different from RA plus UVB-treated cells (p<0.05).

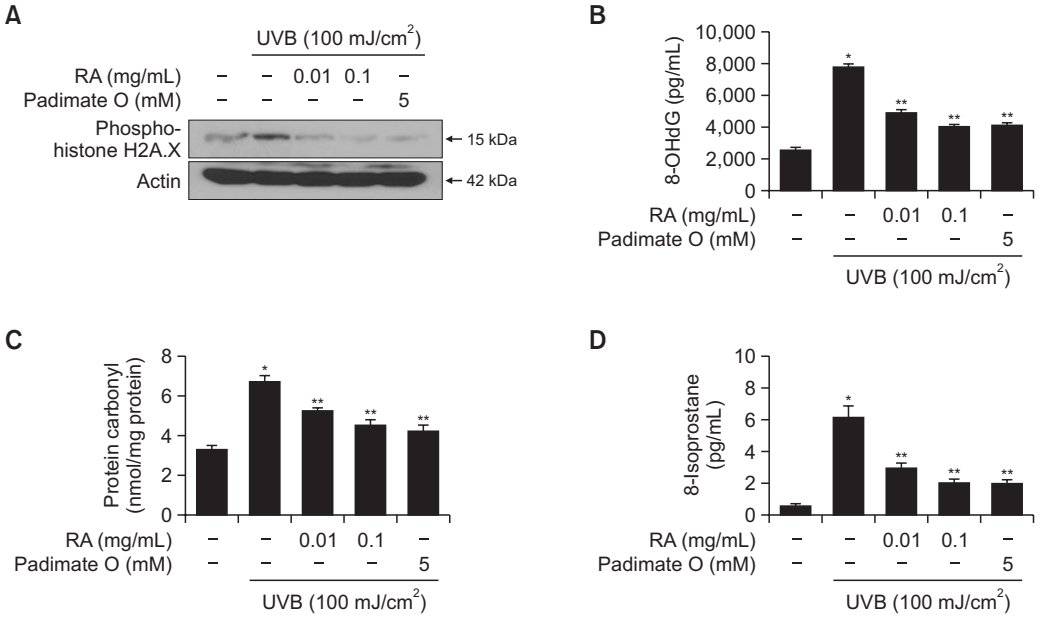

Fig. 5. Rosmarinic acid (RA) inhibits UVB irradiation-induced oxidative damage to components in the dorsal mouse skin tissue. Mice were treated with RA (0.01 or 0.1 mg/mL) or padimate O prior to UVB irradiation. (A) Protein expression of phospho-histone H2A.X, (B) 8-OHdG (indicator of oxidative DNA damage) levels, (C) formation of protein carbonyls (markers of protein oxidation), and (D) 8-isoprostane (marker of lipid peroxidation) levels were assessed. (A) Actin was used as a loading control for phospho-histone H2A.X. (B-D) *Significantly different compared to the non-irradiated control group (p<0.05), and **significantly different compared to the irradiated control group (p<0.05).

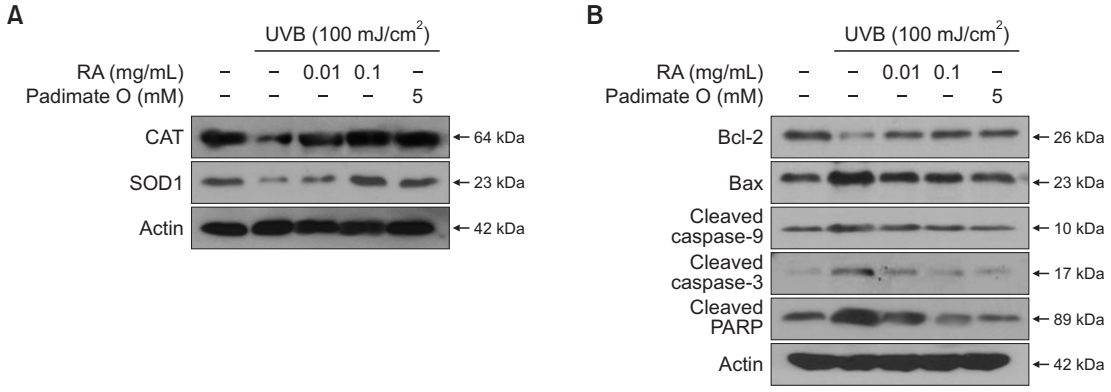

Fig. 6. Rosmarinic acid (RA) inhibits UVB-induced antioxidant enzyme imbalance and apoptosis in the mouse dorsal skin tissue. Mice were administrated with RA (0.01 or 0.1 mg/mL) or padimate O before they were exposed to UVB. (A) Tissue lysates from skin samples were analyzed via western blot to detect the expression of CAT and SOD1. (B) Protein expression of Bcl-2, Bax, cleaved caspase-9 and caspase-3, and cleaved PARP were detected using their specific antibodies. (A, B) Actin was used as a loading control.

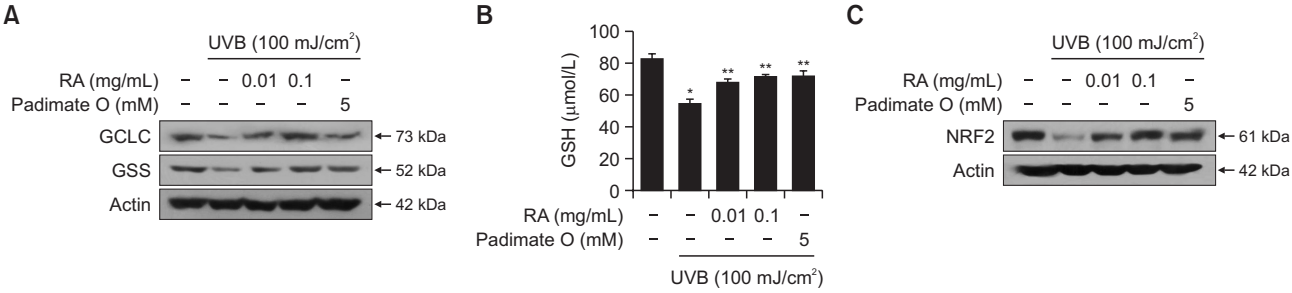

Fig. 7. Effects of rosmarinic acid (RA) on NRF2 and glutathione (GSH) synthesis in response to UVB irradiation in mouse dorsal skin tissue. Mice were coated with RA (0.01 or 0.1 mg/mL) or padimate O before exposure to UVB. Tissue lysates from skin samples were analyzed by western blot to detect the expression of (A) GCLC and GSS using specific antibodies. (B) The GSH level in skin tissues was measured by a GSH detection kit. *Significantly different compared to the non-irradiated control group (p<0.05), and **significantly different compared to the irradiated control group (p<0.05). (C) The expression of NRF2 was detected by western blot analysis using specific antibody. (A, C) Actin was used as a loading control.

lular antioxidant defenses and reverses UVB-induced oxidative damage. However, its role as a potent NRF2 inducer in the skin and its involvement in various signaling pathways remain unclear. In this study, we investigated these aspects and provided novel findings on the mechanisms underlying the antioxidant activities of RA. We demonstrated that RA acts as a potent antioxidant by activating NRF2 translocation into the nucleus. In parallel with NRF2 activation, we showed that RA induces GSH production, which is followed by an enhanced antioxidant defense. The sulfhydryl group (SH) of GSH is readily polarizable and facilitates the removal of free radicals and their derivatives (Gomes *et al*., 2023). Further, tripeptide GSH acts as the cofactor for glutathione peroxidation and is, therefore, involved in the detoxification of electrophilic compounds (Lapenna, 2023). As suppressed GSH levels disturb the cellular antioxidant capacity, the RA-induced increase in GSH content largely enhances the antioxidant status of the skin, thereby protecting against UVB-induced oxidative damage.

AKT is activated by phosphorylation at Thr308 and Ser473 and promotes cell survival and proliferation (Asare *et al*., 2023). The ERK pathway is generally stimulated by the activation of the epidermal growth factor receptor in response to stress stimuli (Chen *et al*., 2016) and induces either cell survival or proliferation. Previous studies using different compounds, such as tert-butyl hydroquinone, eckol, sulforaphane, and fucoxanthin, reported that AKT and ERK functions are essential for NRF2 activation in different cell lines (Qin and Hou, 2016). In the present study, to the best of our knowledge, we showed for the first time that RA activates the AKT and ERK signaling pathways in cultured human keratinocytes. Using two different inhibitors of AKT and ERK (LY294002 or U0126) and specific siRNA, we demonstrated that the inhibition of the AKT and ERK pathways decreased the RA-induced enhanced NRF2 activity and GSH synthesis. Thus, we concluded that the functional PI3K/AKT and ERK pathways are required for the activation of NRF2 and GSH biosynthesis.

In addition, to approach *in vivo* conditions in the *in vitro* setup, we first analyzed mouse tissues with different biomarkers for oxidative damage. RA attenuated UVB-induced oxidative DNA injury, as evidenced by the phosphorylation of H2A.X and 8-OHdG. Moreover, the formation of protein carbonyls via oxidative cleavage of the protein backbone and 8-isoprostanes, which are prostaglandin-like compounds produced from the free radical-mediated peroxidation of essential fatty acids, was reduced by the administration of RA. In addition to these

effects, RA also prevented UVB-induced oxidative damage in mouse skin tissues, as measured by various key markers of apoptosis. Our results in mouse skin dorsal tissue indicated that RA treatment prevents the UVB-induced reduction of NRF2 protein expression, while restoring phase II detoxification and antioxidant enzymes. Moreover, as UVB irradiation resulted in GSH depletion, our present data suggest that RA treatment significantly prevents UVB-induced GSH depletion. Thus, the topical application of RA protects against UVB-induced skin damage in hairless mice, suggesting that RA treatment is a promising approach to protect the skin from oxidative damage in response to UVB radiation.

In summary, the results of the present study suggest that RA protects against UVB-induced oxidative damage by activating AKT and ERK signaling to regulate NRF2 signaling and enhance GSH biosynthesis.

CONFLICT OF INTEREST

The authors declare no conflicts of interest.

ACKNOWLEDGMENTS

This research was supported by the Basic Science Research Program through the National Research Foundation of Korea (NRF) funded by the Ministry of Education (RS-2023-00270936). This work was supported by a research grant from Jeju National University Hospital in 2023.

REFERENCES

Amoah, S. K., Sandjo, L. P., Kratz, J. M. and Biavatti, M. W. (2016) Rosmarinic acid--pharmaceutical and clinical aspects. *Planta Med.* **82**, 388-406.

Asare, O., Ayala, Y., Hafeez, B. B., Ramirez-Correa, G. A., Cho, Y. Y. and Kim, D. J. (2023) Ultraviolet radiation exposure and its impacts on cutaneous phosphorylation signaling in carcinogenesis: focusing on protein tyrosine phosphatases. *Photochem. Photobiol.* **99**, 344-355.

Ashrafizadeh, M., Ahmadi, Z., Mohammadinejad, R., Farkhondeh, T. and Samarghandian, S. (2020) Curcumin activates the Nrf2 pathway and induces cellular protection against oxidative injury. *Curr. Mol. Med.* **20**, 116-133.

Azmanova, M. and Pitto-Barry, A. (2022) Oxidative stress in cancer therapy: friend or enemy? *Chembiochem.* **23**, e202100641.

Chen, J., Zeng, F., Forrester, S. J., Eguchi, S., Zhang, M. Z. and Harris, R. C. (2016) Expression and function of the epidermal growth factor receptor in physiology and disease. *Physiol. Rev.* **96**, 1025-1069.

Farkhondeh, T., Folgado, S. L., Pourbagher-Shahri, A. M., Ashrafizadeh, M. and Samarghandian, S. (2020) The therapeutic effect of resveratrol: Focusing on the Nrf2 signaling pathway. *Biomed. Pharmacother.* **127**, 110234.

Fernando, P. M., Piao, M. J., Kang, K. A., Ryu, Y. S., Hewage, S. R., Chae, S. W. and Hyun, J. W. (2016) Rosmarinic acid attenuates cell damage against UVB radiation-induced oxidative stress via enhancing antioxidant effects in human HaCaT cells. *Biomol. Ther. (Seoul)* **24**, 75-84.

G Bardallo, R., Panisello-Roselló, A., Sanchez-Nuno, S., Alva, N., Roselló-Catafau, J. and Carbonell, T. (2022) Nrf2 and oxidative stress in liver ischemia/reperfusion injury. *FEBS J.* **289**, 5463-5479.

Galicia-Moreno, M., Lucano-Landeros, S., Monroy-Ramirez, H. C., Silva-Gomez, J., Gutierrez-Cuevas, J., Santos, A. and Armendariz-Borunda, J. (2020) Roles of Nrf2 in liver diseases: molecular, pharmacological, and epigenetic aspects. *Antioxidants* **9**, 980.

Gomes, K. K., Dos Santos, A. B., Dos Anjos, J. S., Leandro, L. P., Mariano, M. T., Pinheiro, F. L., Farina, M., Franco, J. L. and Posser, T. (2023) Increased iron levels and oxidative stress mediate age-related impairments in male and female Drosophila melanogaster. *Oxid. Med. Cell. Longev.* **2023**, 7222462.

Gonchar, O. O., Maznychenko, A. V., Klyuchko, O. M., Mankovska, I. M., Butowska, K., Borowik, A., Piosik, J. and Sokolowska, I. (2021) C60 fullerene reduces 3-nitropropionic acid-induced oxidative stress disorders and mitochondrial dysfunction in rats by modulation of p53, Bcl-2 and Nrf2 targeted proteins. *Int. J. Mol. Sci.* **22**, 5444.

He, F., Ru, X. and Wen, T. (2020) NRF2, a transcription factor for stress response and beyond. *Int. J. Mol. Sci.* **21**, 4777.

Ijaz, S., Iqbal, J., Abbasi, B. A., Ullah, Z., Yaseen, T., Kanwal, S., Mahmood, T., Sydykbayeva, S., Ydyrys, A., Almarhoon, Z. M., Sharifi-Rad, J., Hano, C., Calina, D. and Cho, W. C. (2023) Rosmarinic acid and its derivatives: current insights on anticancer potential and other biomedical applications. *Biomed. Pharmacother.* **162**, 114687.

Jena, A. B., Samal, R. R., Bhol, N. K. and Duttaroy, A. K. (2023) Cellular Red-Ox system in health and disease: the latest update. *Biomed. Pharmacother.* **162**, 114606.

Kumar, K. J. S., Vani, M. G. and Wang, S. Y. (2022) Limonene protects human skin keratinocytes against UVB-induced photodamage and photoaging by activating the Nrf2-dependent antioxidant defense system. *Environ. Toxicol.* **37**, 2897-2909.

Lapenna, D. (2023) Glutathione and glutathione-dependent enzymes: from biochemistry to gerontology and successful aging. *Ageing Res. Rev.* **92**, 102066.

Li, G. S., Jiang, W. L., Tian, J. W., Qu, G. W., Zhu, H. B. and Fu, F. H. (2010) *In vitro* and *in vivo* antifibrotic effects of rosmarinic acid on experimental liver fibrosis. *Phytomedicine* **17**, 282-288.

Li, P. F., Xiang, Y. G., Zhang, D., Lu, N., Dou, Q. and Tan, L. (2021) Downregulation of DNA ligases in trophoblasts contributes to recurrent pregnancy loss through inducing DNA damages. *Placenta* **106**, 7-14.

Liu, T., Lv, Y. F., Zhao, J. L., You, Q. D. and Jiang, Z. Y. (2021) Regulation of Nrf2 by phosphorylation: consequences for biological function and therapeutic implications. *Free Radic. Biol. Med.* **168**, 129-141.

Liu, T., Sun, L., Zhang, Y., Wang, Y. and Zheng, J. (2022a) Imbalanced GSH/ROS and sequential cell death. *J. Biochem. Mol. Toxicol.* **36**, e22942.

Liu, Y., Liu, Y., Deng, J., Wu, X., He, W., Mu, X. and Nie, X. (2022b) Molecular mechanisms of marine-derived natural compounds as photoprotective strategies. *Int. Immunopharmacol.* **111**, 109174.

McDaniel, D., Farris, P. and Valacchi, G. (2018) Atmospheric skin aging-contributors and inhibitors. *J. Cosmet. Dermatol.* **17**, 124-137.

Mohamed, S. A. and Hargest, R. (2022) Surgical anatomy of the skin. *Surgery* **40**, 1-7.

Nie, Y., Chu, C., Qin, Q., Shen, H., Wen, L., Tang, Y. and Qu, M. (2023) Lipid metabolism and oxidative stress in patients with Alzheimer's disease and amnestic mild cognitive impairment. *Brain Pathol.* doi: 10.1111/bpa.13202 [Online ahead of print].

Noor, S., Mohammad, T., Rub, M. A., Raza, A., Azum, N., Yadav, D. K., Hassan, M. I. and Asiri, A. M. (2022) Biomedical features and therapeutic potential of rosmarinic acid. *Arch. Pharm. Res.* **45**, 205-228.

Pantelic, M. N., Wong, N., Kwa, M. and Lim, H. W. (2023) Ultraviolet filters in the United States and European Union: a review of safety and implications for the future of US sunscreens. *J. Am. Acad. Dermatol.* **88**, 632-646.

Papaccio, F., D'Arino, A., Caputo, S. and Bellei, B. (2022) Focus on the contribution of oxidative stress in skin aging. *Antioxidants* **11**, 1121.

Piao, M. J., Ahn, M. J., Kang, K. A., Kim, K. C., Cha, J. W., Lee, N. H. and Hyun, J. W. (2015) Phloroglucinol enhances the repair of UVB radiation-induced DNA damage via promotion of the nucleotide excision repair system *in vitro* and *in vivo*. *DNA Repair* **28**, 131-138.

Qin, S. and Hou, D. X. (2016) Multiple regulations of Keap1/Nrf2 system by dietary phytochemicals. *Mol. Nutr. Food Res.* **60**, 1731-

1755.
Rocha, J., Eduardo-Figueira, M., Barateiro, A., Fernandes, A., Brites, D., Bronze, R., Duarte, C. M., Serra, A. T., Pinto, R., Freitas, M., Fernandes, E., Silva-Lima, B., Mota-Filipe, H. and Sepodes, B. (2015) Anti-inflammatory effect of rosmarinic acid and an extract of rosmarinus officinalis in rat models of local and systemic inflammation. *Basic Clin. Pharmacol. Toxicol.* **116**, 398-413.
Vetrani, C., Piscitelli, P., Muscogiuri, G., Barrea, L., Laudisio, D., Graziadio, C., Marino, F. and Colao, A. (2022) Planeterranea: an attempt to broaden the beneficial effects of the Mediterranean diet worldwide. *Front. Nutr.* **9**, 973757.
Wang, J., Deng, H., Zhang, J., Wu, D., Li, J., Ma, J. and Dong, W. (2020) α-Hederin induces the apoptosis of gastric cancer cells accompanied by glutathione decrement and reactive oxygen species generation via activating mitochondrial dependent pathway. *Phytother. Res.* **34**, 601-611.
Wang, R., Liang, L., Matsumoto, M., Iwata, K., Umemura, A. and He, F. (2023) Reactive oxygen species and NRF2 signaling, friends or foes in cancer? *Biomolecules* **13**, 353.
Wei, J., Zhao, Q., Zhang, Y., Shi, W., Wang, H., Zheng, Z., Meng, L., Xin, Y. and Jiang, X. (2021) Sulforaphane-mediated Nrf2 activation prevents radiation-induced skin injury through inhibiting the oxidative-stress-activated DNA damage and NLRP3 inflammasome. *Antioxidants* **10**, 1850.